Filter-Free Wavelength Conversion Using Mach-Zehnder Interferometer with Integrated Multimode Interference Semiconductor Optical Amplifiers

Jong-Hoi Kim, Hyun-Soo Kim, Eun-Deok Sim, Kang-Ho Kim,
Oh-Kee Kwon, and Kwang-Ryong Oh

We propose a filter-free wavelength conversion using a Mach-Zehnder interferometer with monolithically integrated 2×2 multimode interference semiconductor optical amplifiers (MMI-SOAs). The device has been optimized by considering a non-homogeneous carrier distribution due to the self-imaging properties of the MMI-SOA. Static measurements show an extinction ratio of up to 18 dB and an input signal rejection ratio of up to 20 dB.

Keywords: Wavelength conversion, semiconductor optical amplifier, March-Zehnder interferometer, cross-phase modulation.

Manuscript received Nov. 6, 2003; revised May 6, 2004.

The research featured in this paper is supported by Korean Ministry of Information and Communication (MIC).

Jong-Hoi Kim (phone: +82 42 860 6943, email: jonghoi@etri.re.kr), Hyun-Soo Kim (email: kimhyunsoo@etri.re.kr), Eun-Deok Sim (email:sed63252@etri.re.kr), Kang-Ho Kim (email: kkh63261@etri.re.kr), Oh-Kee Kwon (email: okkwon@etri.re.kr), and Kwang-Ryong Oh (email: kroh@etri.re.kr) are with Basic Research Laboratory, ETRI, Daejeon, Korea.

I. Introduction

All-optical wavelength conversion will be a key function for future wavelength division multiplexed networks, as it allows for a flexible and distributed network management [1]. Mach-Zehnder interferometric wavelength converters (MZI-WCs) based on cross-phase modulation in a semiconductor optical amplifier (SOA) have provided high-speed operation at 10 Gb/s or over [2], [3]. In such co-propagation for high-speed conversion, filter-free operation is essential to allow cascade integration or conversion to the same wavelength [4]. All-active dual-order mode wavelength conversion has been demonstrated with high-input signal rejection using multimode interference couplers (MMIs) [5]. An MMI is useful in spatially processing optical fields, allowing field splitting/dividing or mode conversion. Recently, this feature has assisted active devices in improving their performances and developing a new functional device. An active 1×1 MMI has been proposed that provides high-input saturation power owing to a wider pumping area than a conventional SOA with a single-mode waveguide [6]. The 2×2 MMI-SOA has been applied to demonstrate all-optical 2R regeneration, allowing a digital transfer characteristic and a high increase in the extinction ratio [7]. In this paper, we describe the principle of filter-free wavelength conversion based on a 2×2 MMI-SOA in a Mach-Zehnder interferometer and the fabrication of monolithically integrated MZI-WCs. We also introduce a modified beam propagation method for optimization of the MMI-SOA in order to consider a non-homogeneous carrier

distribution due to the self-imaging properties. And, we show the theoretical analysis and experimental results for static characteristics.

II. Design

An input signal is propagated to an absorber in one output port of the 2×2 MMI-SOA while the continuous wave (CW) passes through the other output port as shown Fig. 1. Thus, filter-free wavelength conversion can be achieved by rejecting the input signal in the absorber and is characterized by an input signal rejection ratio, defined as a power ratio of the converted signal to the input signal at the output of the device. In order to improve the input signal rejection ratio, the width and length of the MMI-SOA are optimized for the cross-state using self-imaging properties of the input field.

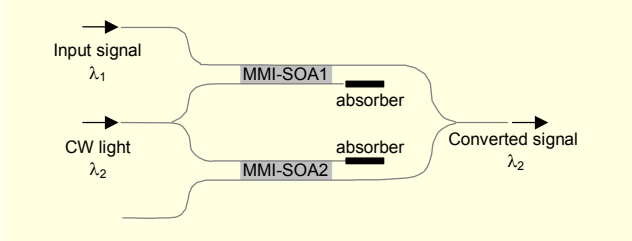

Fig. 1. Schematic diagram of the filter-free MZI-WC using 2×2 MMI-SOAs.

The carrier dynamics in the 2×2 MMI-SOA can be analyzed by using a modified beam propagation method (BPM) based on a conventional BPM [8] and an SOA model segmented into smaller sections than the cavity length [9], [10]. Here, the section length for the SOA model is equivalent to the mesh size for the finite-difference BPM. An optimization of the MMI-SOA is performed using a beam propagation method incorporating a traveling wave rate equation, which considers a non-homogeneous distribution of the refractive index associated with changes in the carrier density due to the locally distributed field profile. The carrier density in each section for the multi-wave coupled into the SOA is evaluated by using the rate equation,

$$\frac{dN_i}{dt} = \frac{I}{qV} - R_i - \sum_{k=1,2} g_{k,i} v_g S_{k,i} - a(N_i - N_0) v_g S_{t,i}\ , \quad (1)$$

where subscripts k and i denote the input channel number and section number, I is the bias current, q is the electron charge, d is the volume of the active region, a is the gain factor, N_0 is the carrier density at transparency, v_g is the group velocity associated with group index n_g and is taken to be c/n_g, and R_i is the recombination rate given by

$$R_i = c_1 N_i + c_2 N_i^2 + c_3 N_i^3, \quad (2)$$

where c_1, c_2, and c_3 are constants. The third term in (1) accounts for the stimulated emission by the input signal and the CW light where $S_{k,i}$ is the average photon density. Assuming the parabolic gain spectrum, material gain $g_{k,i}$ is given by [11]

$$g_{k,i} = a(N_i - N_0) - \gamma\left[\lambda_k - \lambda_p + \frac{d\lambda}{dN}(N_i - N_p)\right]^2, \quad (3)$$

where γ is the gain factor, λ_k is the signal wavelength, λ_p is the peak gain wavelength at the reference carrier density, N_p, and $d\lambda/dN$ is the wavelength shift coefficient with the carrier density. The last term in (1) accounts for the spontaneous emission where $S_{t,i}$ is the average photon density and can be obtained from the model based on [12]. The nonlinear phase change, arising from carrier density-induced changes in the refractive index, is given by [13]

$$\Delta\phi_i = \frac{2\pi L_i}{\lambda_k}\Gamma(N_i - N_0)\frac{dn}{dN}, \quad (4)$$

where L_i is the section length, Γ is the confinement factor, and dn/dN, which is taken to be constant, is the rate of change of the active region refractive index with the carrier density.

The device structure used in the experiment is a typical buried heterostructure in order to avoid the spreading of the lateral current by confining the injected current. For this structure, the lateral profile of the carrier density in the MMI-SOA is mainly determined by surface recombination at the edges of the active layer rather than by lateral carrier diffusion [14]. The surface recombination is assumed to be lower than 1×10^4 cm/s, which is a typical value for an InGaAsP-InP system [15], because the additional wet-etching steps have been introduced in the fabrication process in order to decrease the dry-etching damage. For values lower than 10^4 cm/s, the influence on the self-imaging behavior is negligible. However, a theory including surface recombination needs to be developed in order to accurately predict the characteristics of the device.

Figure 2 shows calculated light intensity patterns in the filter-free MZI-WC, with and without the input signal. The CW light experiences constructive or destructive interference depending on the phase shift through the MMI-SOAs. The 2×2 MMI-SOA is optimized with the cross-state in order to provide a shorter device and thus avoid a high injection current. The refractive index in the local region with the higher intensity is higher than that of the surroundings due to carrier depletion. This nonlinear effect influences the behavior of the MMI-SOA due to a change in the self-imaging distance.

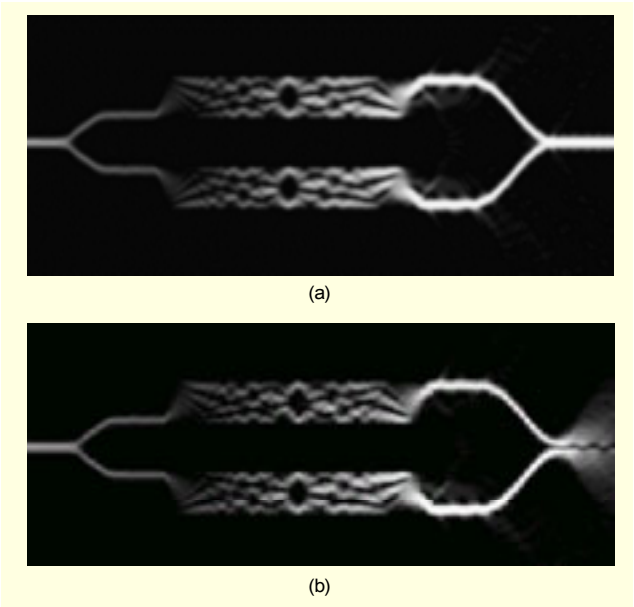

Fig. 2. Calculated intensity patterns of the CW light in the MZI-WC (a) without the input signal and (b) with the input signal of 0 dBm.

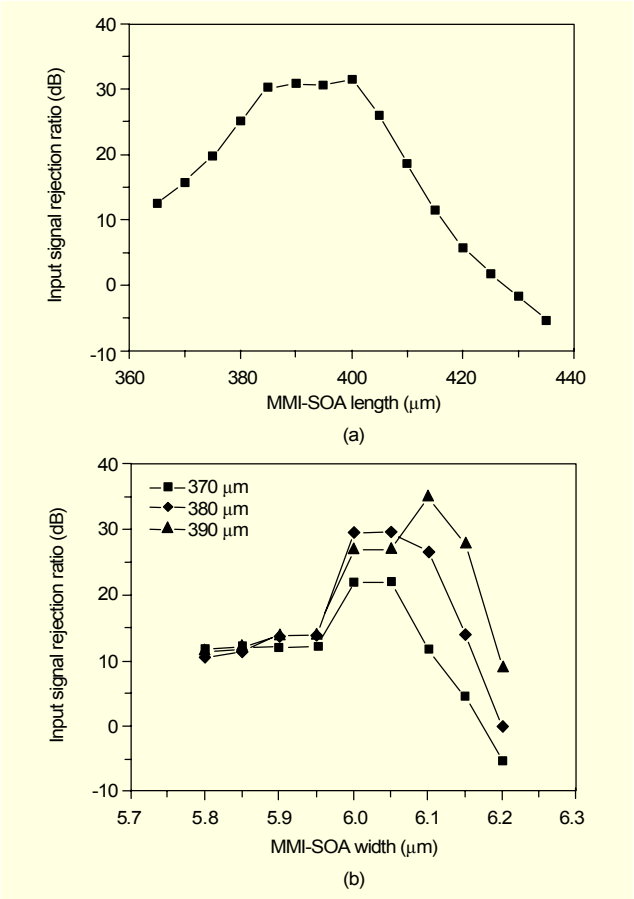

Fig. 3. Dependences of the input signal rejection ratio on (a) the length for a 6-μm wide 2 × 2 MMI-SOA and (b) the width for 2 × 2 MMI-SOAs.

Figure 3 shows the theoretical results for the input signal rejection ratio with the width of the MMI-SOA. It gives both the length and width tolerances as well as the optimized length and width. The width tolerance is 0.2 μm for an input signal rejection ratio of 20 dB.

III. Fabrication

The active and passive structures and a fabricated chip of monolithically integrated MZI-WCs with 380-μm long 2×2 MMI-SOAs are shown in Figs. 4 and 5. The MMI-SOAs were designed with widths from 5.9 to 6.1 μm by 0.1-μm steps. The MMI-SOA consists of a 0.15-μm-thick bulk InGaAsP (λ_g = 1.55 μm) active layer sandwiched by two 0.1-μm thick InGaAsP (λ_g = 1.15 μm) separate confinement hetero-structure layers and caped by a 0.3-μm thick p-doped InP. We grew the active layer structure using metal-organic chemical vapor deposition growth. After the active layers in the passive region were dry etched using reactive ion etching, a 0.4-μm thick InGaAsP (λ_g = 1.24 μm) core and a 0.3-μm thick InP cladding layer were butt-jointed. The MMI and passive waveguide was formed by reactive ion etching and embedded using a p-doped InP cladding layer and InGaAs contact layer. A selective wet etching with a depth of 3 μm and the growth of an undoped InP were performed outside the MMI-SOA. The undoped InP is utilized to form a current blocking layer of the MMI-SOA and a cladding layer of the passive waveguide. We note that this process forms a current blocking layer without conventional ion implantation and an undoped InP cladding layer for reducing the propagation loss due to absorption in a p-doped InP cladding layer, simultaneously. The input and output waveguides are tilted by 7°, and the antireflection coating of a TiO_2/SiO_2 double layer is applied to the facet. The length and width of the chip are 4.8 and 1mm.

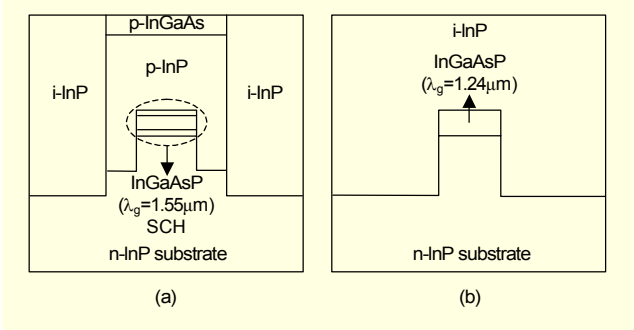

Fig. 4. Schematic cross-sectional view of (a) the SOA and (b) the passive waveguide structure.

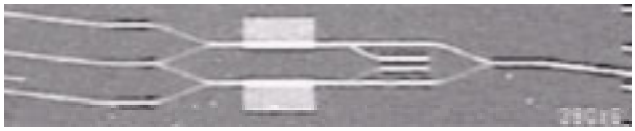

Fig. 5. Photograph of the fabricated MZI-WC chip.

IV. Results and Discussion

The CW light at a wavelength of 1550 nm is injected into the MZI-WC and intensity-modulated at the output by constructive or destructive interference depending on the phase difference between the MMI-SOAs. The phase shift can be controlled by the bias currents injected into the MMI-SOAs. Figure 6 shows the experimental and theoretical results for an output power with the bias current injected into the MMI-SOA. The interference transfer function provides the ratio between a constructive and destructive interference of up to 18 dB. The current levels of the off state of the theory and of the experiment have a difference of 3 mA. As mentioned above, it is possible to decrease the difference by considering the lateral perturbation of the carrier density due to the surface recombination in the buried heterostructure. In addition, the output power levels at high currents of over 120 mA in the theory are higher than those in the experiment. The lower output power levels in the experiment are caused by the gain degradation associated with the fact that the threshold current increases for an increasing temperature. The optical losses originate from the propagation loss in the passive waveguide and the coupling loss between the optical fiber and the chip due to the absence of the spot-size converter. The coupling loss of up to 8 dB is determined by fitting the calculated data to the experimental result. The propagation loss of 5.7 dB/cm in the waveguide was measured using a low-coherence interferometric reflectometer. The additional losses are the 3-dB losses in the Y-junctions of the waveguide. As a result, the total loss in the device is up to 28 dB. Figure 7 shows the polarization dependency of the CW light measured using the same device. Output power as a function of the injected current for TE mode is higher than

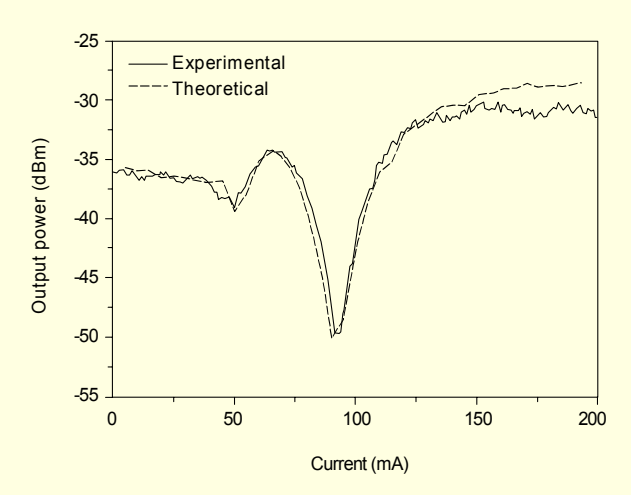

Fig. 6. Experimental and theoretical variations of the output power with an injection current into the MMI-SOA1. MMI-SOA2 = 100 mA, CW power = 0 dBm.

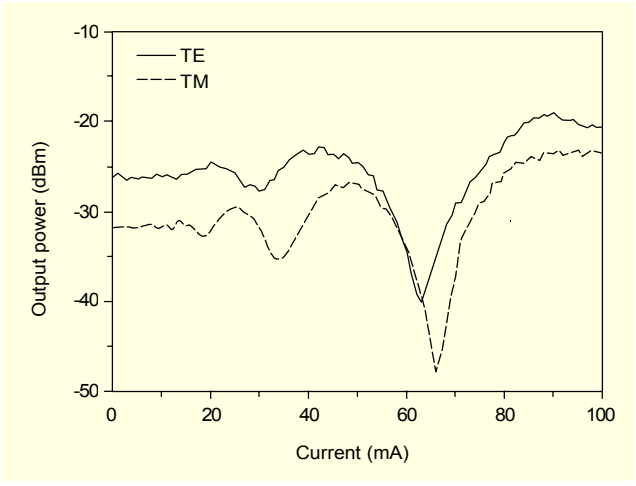

Fig. 7. Measured polarization dependency of the CW light for the MZI-WC with the MMI-SOAs. MMI-SOA2 = 100 mA, CW power = 0 dBm.

that for TM mode. The active layer of the MMI-SOA has a layer structure optimized for a polarization-independent SOA with a tensile-strained bulk InGaAsP. This structure results in a higher gain in TE mode, with a difference of 1 dB in the extinction ratio, and a difference of 2 mA in the injected current for the minimum output power. It is possible to provide the polarization-independent characteristics of the MMI-SOA integrated Mach-Zehnder interferometer by optimizing the strained bulk InGaAsP for a wider SOA than the stripe width of a single-mode SOA.

The input signal at a wavelength of 1545 nm is co-propagated in the device and rejected by the absorber in the output port of the MMI-SOA. We measured the optical spectrum to investigate the input signal rejection ratio. The optical inputs have been coupled into the MZI-WC chip using lensed fibers in the input and output ports. The input signal rejection ratio is obtained by sending the optical inputs to an optical spectrum analyzer to measure the difference between the powers at two wavelengths of the input signal and the CW light in a bandwidth of 0.1 nm. Figure 8(a) shows an input signal rejection ratio of 20 dB for the co-propagation of the input signal and CW light. As shown in Fig. 3, the input signal rejection ratio is mainly dependent on the width of the 2 × 2 MMI-SOA, and thus the filter-free operation is strongly dependent on the width. We investigated the width dependence of the input signal rejection ratio by fabricating the MMI-SOAs with width variations in steps of 0.1 μm. Figure 8(b) shows a degradation of 12 dB in the input signal rejection ratio for width variations of 0.2 μm. Pattern broadening in photo-lithography leads to the difference in the optimized width in both the theory and in our experiment.

The wavelength ranges for the filter-free operation were

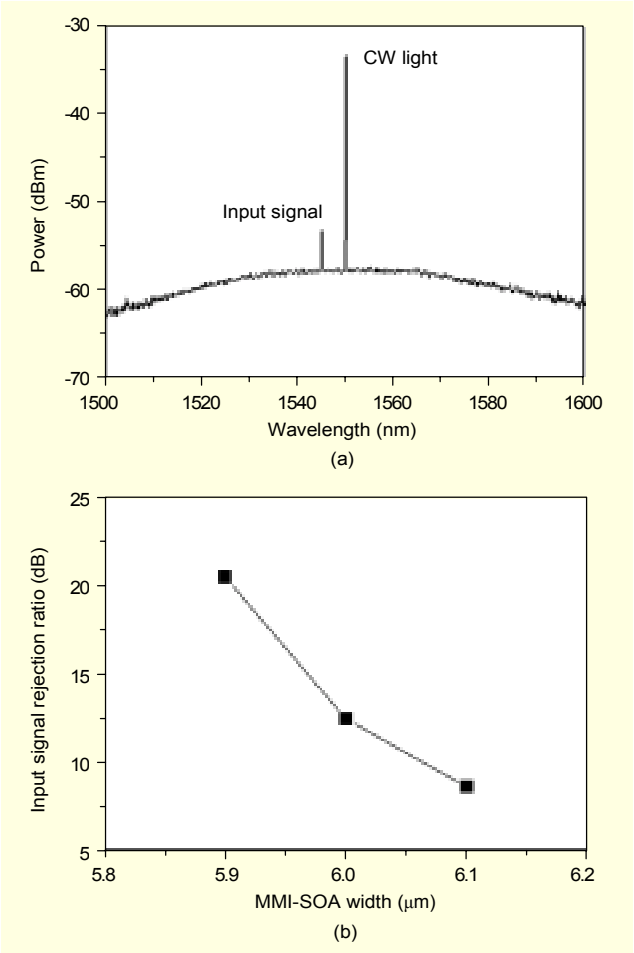

Fig. 8. Output spectrum and measured input signal rejection ratio for co-propagation of the input signal and CW light. MMI-SOA1 = 100 mA, MMI-SOA2 = 100 mA, CW power = 0 dBm.

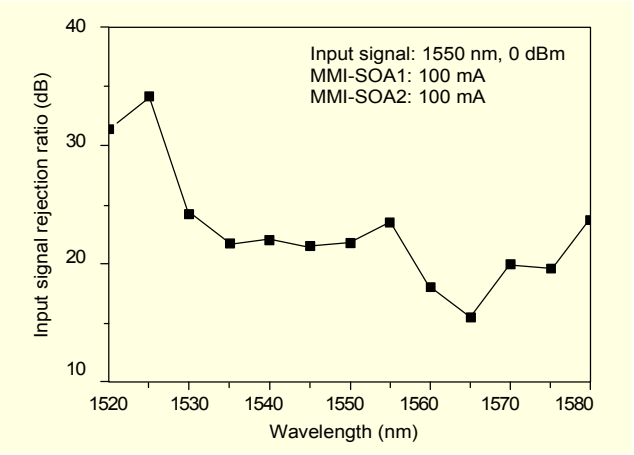

Fig. 9. The measured spectral bandwidth of the MZI-WC with the MMI-SOAs.

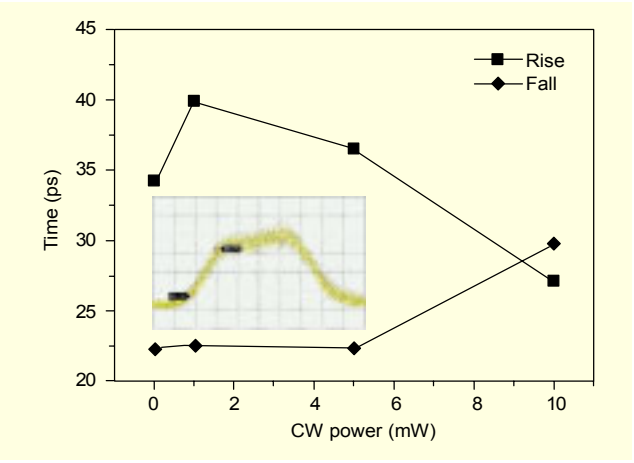

Fig. 10. The measured rise and fall time with CW power. MMI-SOA1 = 100 mA, MMI-SOA2 = 100 mA. The inset shows a waveform of the input signal at 10 Gbit/s for a CW power of 10 dBm.

investigated by coupling the CW light (1520 to 1580 nm, 0 dBm) into the MMI-SOA-integrated MZI-WC, as shown in Fig. 8. The input signal rejection ratio is strongly dependent on the transmittance of the input signal. The length of the MMI-SOA is shorter than the optimized length due to the pattern broadening in photo-lithography, as mentioned above. In general, as a wavelength of an input light is shorter, the optimized length of an MMI coupler is longer. Thus, the input signal rejection ratio is higher in the shorter wavelength of the CW light. The bandwidth is strongly dependent on the wavelength, and the dependency of the bandwidth on the wavelength needs to be investigated for the optimized device. The spectral bandwidth for an input signal rejection ratio over 20 dB is about 35 nm (1520 to 1555 nm). We expect that the spectral bandwidth is wider than 35 nm if the MMI-SOA is optimized.

In order to investigate the dynamic properties of the 2×2 MMI-SOA, when an input signal of 10 Gb/s at 1550 nm and a CW light at 1545 nm were injected into the MMI-SOA in a counter-propagating operation, the rise/fall times of the output signal at 1550 nm were measured using the input power of the CW light, as shown in Fig. 9. In the counter-propagation, the higher power level of the CW light leads to the shorter rise time and longer fall time. Significant degradation in the rise/fall time does not occur. This is because the overlap of the input signal and the CW light in the MMI-SOA is smaller than in a long SOA and thus the lights do not experience a strong saturation of the carrier density. However, the carrier density in the long SOA will be lower in the part of the SOA where the CW light enters since the amplified input signal that comes from the opposite direction causes a strong saturation. Thus, we suppose that an MMI-SOA does not need to be the same length in order to have same recovery times of the SOA.

A conventional MZI-WC with an SOA of longer than 1200

μm has speed limitations in the counter-propagation coupling scheme since only co-propagation of the input signal and the CW light can be used due to the large transit time of the long SOAs and the conventional MZI-WC's narrower wavelength span due to the spectral bandwidth shrinking as the cavity length increases. In the MZI-WCs with MMI-SOAs, counter-propagation is available using the 2 × 2 MMI-SOAs with a bar-state. Note that the available span for the spectral bandwidth is wider than MZI-WCs with long SOAs since the MMI-SOA is shorter than the conventional SOA.

V. Conclusion

We have proposed an MZI configuration with 2 × 2 MMI-SOAs for filter-free wavelength conversion and fabricated a monolithically integrated MZI-WC. We have optimized the MMI-SOA using a modified BPM incorporating the traveling wave rate equation. Static measurements have shown the interferometer property to have an extinction ratio of 18 dB and the filter-free operation to have an input signal rejection ratio of 20 dB for co-propagation.

References

[1] S.J.B. Yoo, "Wavelength Conversion Technologies for WDM Network Applications," *J. Lightwave Technol.*, vol.14, 1996, pp. 955-966.

[2] T. Fjelde, D. Wolfson, P.B. Hansen, A. Kloch, C. Janz, A. Coquelin, I. Guillemot, F. Gaborit, F. Poingt, B. Dagens, and M. Renaud, "20Gbit/s Optical Wavelength Conversion in All-Active Mach-Zehnder Interferometer," *Electron. Lett.*, vol. 35, May 1999, pp. 913-914.

[3] M. Dülk, St. Ficher, E. Gamper, W. Vogt, E. Gini, H. Mechior, W. Hunziker, H.N. Poulsen, A.T. Clausen, A. Buxens, and P. Jeppesen, "Efficient Regenerative Wavelength Conversion at 10Gbit/s over C- and L-Band (80nm span) Using a Mach-Zehnder Interferometer with Monolithicaaly Integrated Semiconductor Optical Amplifiers," *Electron. Lett.*, vol. 36, 2000, pp. 241-243.

[4] C. Janz, F. Poingt, F. Pommereau, F. Gaborit, D. Ottenwalder, I. Guillemot, B. Dagens, and M. Renaud, "All-Active Dual-Order Mode Mach-Zehnder Wavelength Converter for Co-Propagative Operation," *Electron. Lett.*, vol. 34, Sep. 1998, pp. 1848-1849.

[5] C. Janz, F. Poingt, F. Pommereau, W. Grieshaber, F. Gaborit, D. Leclerc, I. Guillemot, and M. Renaud, "All-Active Dual-Order Mode (DOMO) Mach-Zehnder Wavelength Converter for 10 Gbit/s Operation," *Electron. Lett.*, vol. 35, Oct. 1999, pp. 1862-1863.

[6] K. Hamamoto, E. Gini, C. Holtmann, H. Melchior, S. Sudo, K. Mori, T. Sasaki, and M. Yamaguchi, "Active Multi-Mode-Interferometer Semiconductor Optical Amplifier," *Electron. Lett.*, vol. 36, July 2000, pp. 1218-1220.

[7] J. De Merlier, G. Morthier, S. Verstuyft, T. Van Caenegem, I. Moermen, P. Van Daele, and R. Baets, "Experimental Demonstration of All-Optical Regeneration Using an MMI-SOA," *IEEE Photon. Technol. Lett.*, vol. 14, May 2002, pp. 660-662.

[8] Y. Chung and N. Dagli, "Analysis of z-Invariant and z-Variant Semiconductor Rib Waveguides by Explicit Finite Difference Beam Propagation Method with Nonuniform Mesh Configuration," *IEEE J. Quantum Electron.*, vol.27, 1991, pp. 2296-2305.

[9] J. Kim, K. Oh, and K. Cho, "Spectral Characteristics of Optical Pulse Amplifications with a Holding Light in Semiconductor Optical Amplifiers," *Opt. Comm.*, vol. 170, 1999, pp. 99-109.

[10] J. Kim, K. Oh, H. Kim, and K. Cho, "All-Optical Switching by Counterpropagating Operation in Cascaded Semiconductor Optical Amplifiers," *IEEE Photon. Technol. Lett.*, vol. 12, 2000, pp. 513-515.

[11] J. Wang, H. Olesen, and K. Stubkjaer, "Recombination, Gain and Bandwidth Characteristics of 1.3 μm Semiconductor Laser Amplifiers," *J. Lightwave Technol.*, vol. LT-5, 1987, pp. 184-189.

[12] T. Durhuus, B. Mikkelsen, and K.E. Stubkjaer, "Detailed Dynamic Model for Semiconductor Optical Amplifiers and their Crosstalk and Intermodulation Distortion," *J. Lightwave Technol.*, vol. 10, 1992, pp. 1056-1065.

[13] H. Kawaguchi, "Absorption and Dispersive Bistability in Semiconductor Injection Lasers," *Opt. Quantum Electron.*, vol. 19, 1987, pp. S1-S36.

[14] S.Y. Hu, S.W. Corzine, K.–K. Law, D.B. Young, A.C. Gossard, L.A. Coldren, and J.L. Merz, "Lateral Carrier Diffusion and Surface Recombination in InGaAs/AlGaAs Quantum-Well Ridge-Waveguide Lasers," *J. Appl. Phys.*, vol. 76, 1994, pp. 4479-4487.

[15] T. Baba, F. Koyama, and K. Iga, "Strong Enhancement of Light Extraction Efficiency in GaInAsP 2-D-Arranged Microscolums," *J. Lightwave Technol.*, vol. 17, 1999, pp. 2113-2119.

Jong-Hoi Kim received the BS, MS, and PhD degrees in physics from Sogang University, Korea, in 1993, 1995, and 2000. In 2000, he joined the Basic Communication Research Laboratory of Electronics and Telecommunications Research Institute (ETRI) where he is engaged in work on all-optical functional devices based on semiconductor optical amplifiers, such as all-optical wavelength converters and all-optical gate switches.

Hyun-Soo Kim received the BS, MS, and PhD degrees in material science and engineering from Korea University, Korea, in 1995, 1997, and 2001. In 2001, he joined the Basic Communication Research Laboratory of Electronics and Telecommunications Research Institute (ETRI) where he is engaged in work on all-optical functional devices and photonic integrated circuits based on semiconductor optical amplifiers, such as all-optical wavelength converters and DFB LD.

Eun-Deok Sim received the BS, MS, and PhD degrees in physics from Yonsei University, Korea, in 1994, 1996, and 2001. He joined the Basic Research Laboratory of ETRI in 2001 and has worked on InP-based optoelectronic devices.

Kang-Ho Kim received the BS and MS degrees in physics from Dong A University, Korea, in 1994 and 1996. He is in a doctoral course at University of Ulsan. In 2001, he joined the Basic Communication Research Laboratory of Electronics and Telecommunications Research Institute (ETRI) where he is engaged in work on WDM devices based on semiconductor lasers, such as wavelength tunable lasers.

Oh-Kee Kwon received the BS and MS degrees in electronic engineering from Hanyang University, Korea, in 1996 and 1998. From 1998 to 2001, he served as an officer in Republic Of Korea Air Force. In 2002, he joined the Basic Communication Research Laboratory of Electronics and Telecommunications Research Institute (ETRI) where he is engaged in work on broadband tunable laser diodes.

Kwang-Ryong Oh joined the Electrical and Telecommunications Research Institute (ETRI), Daejeon, Korea, as a Researcher in 1985, where he was involved in the characterization and development of long wavelength semiconductor lasers and PIN + JFET OEIC. Since 1992, he had been involved in the area of the optical switches such as TIR and LD gate optical switches. His current research areas are the WDM optical devices such as SOAs, wavelength converters, and tunable laser diodes.